

# Temperature - pressure phase diagram of the superconducting iron pnictide LiFeP

K. Mydeen,<sup>1,\*</sup> E. Lengyel,<sup>1</sup> Z. Deng,<sup>2</sup> X. C. Wang,<sup>2</sup> C. Q. Jin,<sup>2</sup> and M. Nicklas<sup>1,†</sup>

<sup>1</sup>Max Planck Institute for Chemical Physics of Solids, 01187 Dresden, Germany

<sup>2</sup>Institute of Physics, Chinese Academy of Sciences - Beijing, China

(Dated: November 2, 2018)

Electrical-resistivity and magnetic-susceptibility measurements under hydrostatic pressure up to  $p \approx 2.75$  GPa have been performed on superconducting LiFeP. A broad superconducting (SC) region exists in the temperature - pressure ( $T - p$ ) phase diagram. No indications for a spin-density-wave transition have been found, but an enhanced resistivity coefficient at low pressures hints at the presence of magnetic fluctuations. Our results show that the superconducting state in LiFeP is more robust than in the isostructural and isoelectronic LiFeAs. We suggest that this finding is related to the nearly regular  $[\text{FeP}_4]$  tetrahedron in LiFeP.

PACS numbers: 74.70.Xa, 74.62.Fj, 74.25.Dw

The recently discovered iron-based superconductors attract a great deal of interest because of their high critical temperatures up to  $T_c = 55$  K.<sup>1-7</sup> Soon after the discovery of superconductivity in the iron and nickel based oxyphosphides,  $\text{LaFePO}$ <sup>1</sup> and  $\text{LaNiPO}$ ,<sup>2</sup> superconductivity was found in  $\text{LaFeAsO}_{0.89}\text{F}_{0.11}$  (“1111” type) with a critical temperature of about 26 K.<sup>3</sup> Furthermore, the application of hydrostatic pressure leads to an increase of  $T_c$  up to 43 K at about 4 GPa.<sup>8</sup> The superconductivity in iron-pnictide compounds is closely related to their layered structure, where the iron-pnictide layers are interlaced with charge reservoir layers. Electron or hole doping, both inside and outside of the iron-pnictide layers, strongly affects the superconducting properties.

The effect of external pressure on the structural and electronic properties of the iron-based superconductors can be subtle. In  $\text{La}(\text{O}_{1-x}\text{F}_x)\text{FeAs}$  and  $\text{Sm}(\text{O}_{1-x}\text{F}_x)\text{FeAs}$  the application of pressure revealed an anisotropic lattice compressibility at low pressures,<sup>9</sup> which results in a significant modification of electronic density of states (DOS). In optimally doped  $\text{La}(\text{O}_{1-x}\text{F}_x)\text{FeAs}$   $T_c$  decreases linearly with increasing pressure up to 30 GPa. This decrease is accompanied by the lattice properties becoming less anisotropic.<sup>10</sup> The close connection between structural properties and superconductivity is further shown in  $\text{ReFeAsO}_{1-x}$  ( $\text{Re} =$  rare-earth metal). Here,  $T_c$  attains its maximum value where the  $[\text{FeAs}_4]$  units form a regular tetrahedron.<sup>11,12</sup> In  $\text{Ba}(\text{Fe}_{0.92}\text{Co}_{0.08})_2\text{As}_2$  (“122” type) the uniaxial pressure dependencies of  $T_c$  are highly anisotropic and quite pronounced.<sup>13</sup>  $T_c$  is anticipated to increase with increasing  $c/a$  ratio.

Superconductivity was reported in the “111”-type materials  $\text{LiFeAs}$ <sup>14-16</sup> and  $\text{NaFeAs}$ .<sup>17</sup> In contrast to the “1111” and “122” compounds and to the isostructural  $\text{NaFeAs}$  no signature of a spin-density-wave (SDW) or structural transition has been observed in  $\text{LiFeAs}$  regardless of having a similar charge density in the FeAs layers.<sup>18-21</sup> Recently, Deng *et al.* discovered superconductivity below 6 K in the As free “111” compound  $\text{LiFeP}$ ,<sup>22</sup> which is isostructural and isoelectronic to  $\text{LiFeAs}$  and can be considered as compressed  $\text{LiFeAs}$ . The occurrence

of bulk superconductivity in both stoichiometric  $\text{LiFeAs}$  and  $\text{LiFeP}$  makes them special among the iron-pnictide materials. So far bulk superconductivity in a stoichiometric member of the iron-arsenides and its isostructural phosphorous homolog has not been reported to the best of our knowledge. External pressure and isoelectronic chemical substitution have a different effect on the crystal structure.<sup>22,23</sup> This allows for a detailed study of the influence of structural properties on superconductivity. In this paper we study the effect of hydrostatic pressure on  $\text{LiFeP}$  by electrical-resistivity ( $\rho$ ) and magnetic-susceptibility ( $\chi_{AC}$ ) experiments.

$\text{LiFeP}$  polycrystals were synthesized as described in Deng *et al.*<sup>22</sup>. We carried out four-probe electrical-resistivity and AC-susceptibility measurements under hydrostatic pressure using a physical property measurement system (PPMS, Quantum Design) and a commercial flow cryostat, respectively, utilizing a LR700 resistance/mutual inductance bridge (Linear Research). A compensated coil system placed outside of the pressure cell was used for the AC-susceptibility experiments. Pressures up to 2.75 GPa were generated using a double-layer piston-cylinder type pressure cell. Silicone fluid served as pressure transmitting medium. The pressure was determined at low temperatures by monitoring the pressure-induced shift of the superconducting transition temperature of lead placed close to the sample. The narrow width of the transition confirmed the good hydrostatic pressure conditions inside the cell.

The temperature dependence of the electrical resistivity of  $\text{LiFeP}$  at three representative pressures is depicted in Fig. 1. In the normal state  $\rho(T)$  exhibits a good metallic behavior with no evidence for a SDW instability which is found in many of the “1111”- or “122”-type iron-pnictide materials. A residual resistivity ratio  $RRR = \rho_{300\text{K}}/\rho_0 \approx 43$  at atmospheric pressure confirms the good quality of our polycrystalline sample. Here,  $\rho_{300\text{K}}$  is the resistivity at 300 K and  $\rho_0$  the residual resistivity. At low temperatures, a sharp decrease of  $\rho(T)$  to zero marks the onset of superconductivity, which is observed in the whole investigated pressure range ( $p \leq 2.75$  GPa). The low-temperature normal-

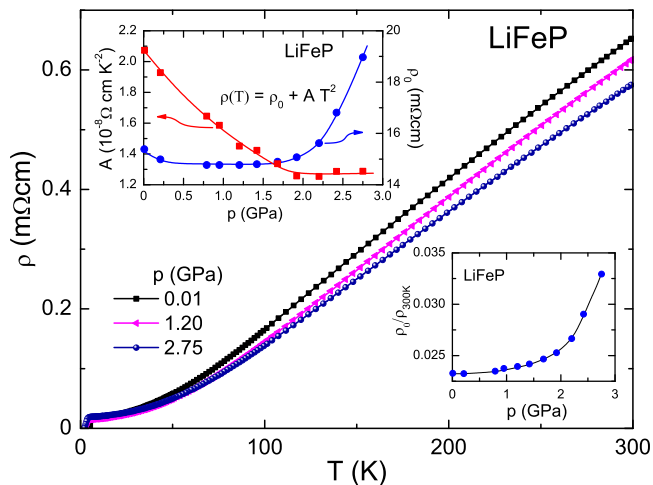


FIG. 1: Electrical resistivity,  $1.8 \text{ K} \leq T \leq 300 \text{ K}$ , of LiFeP for three representative pressures. The upper inset depicts the pressure dependence of the residual resistivity  $\rho_0$  and the prefactor  $A$  obtained from a fit of  $\rho(T) = \rho_0 + AT^2$  to the low-temperature normal-state resistivity. Details are given in the text. The lower inset displays the pressure dependence of the ratio  $\rho_0/\rho_{300\text{K}}$ , where  $\rho_{300\text{K}}$  is the resistivity at  $T = 300 \text{ K}$ .

state resistivity follows a  $T^2$  dependence at all pressures indicating a Fermi-liquid state. The pressure dependence of the parameters  $\rho_0$  and  $A$  of a  $\rho(T) = \rho_0 + AT^2$  fit to the data ( $T_c \leq T \leq 15 \text{ K}$ ) is presented in the upper inset of Fig. 1. The observation of a  $T^2$  behavior at such elevated temperatures hints at the presence of strong electronic correlations. The temperature coefficient  $A$  is a measure of the quasiparticle - quasiparticle (QP - QP) scattering rate.  $A(p)$  decreases by a factor of 1.6 from atmospheric pressure to  $p = 2 \text{ GPa}$  and stays constant with further increasing pressure, indicating a reduction of the QP - QP scattering rate for  $p \leq 2 \text{ GPa}$ . The enhanced QP - QP scattering rate at low pressures might be a hint for the presence of spin fluctuations and indicate the proximity of LiFeP to magnetic order at ambient pressure despite no direct evidence for long-range magnetic order has been found neither in LiFeP nor in its homolog LiFeAs.

At ambient pressure, we find the onset of the resistive transition at about  $\approx 6 \text{ K}$  in good agreement with the literature.<sup>22</sup> Further on, we will use the  $\rho(T) = 0$  criterion to define  $T_c$  from our resistivity data. With increasing pressure the superconducting transition shifts to lower temperatures (see Fig. 2). The width of the transition is nearly pressure independent up to  $p \approx 2.25 \text{ GPa}$ , even though the onset becomes more rounded before a noticeable broadening becomes evident. The significant broadening is accompanied by an increase of the low temperature normal-state resistivity, which is basically pressure independent below  $p \approx 2 \text{ GPa}$ . This behavior is intrinsic to the sample and not caused by, e.g. cracks in the sample, since the room-temperature resistivity,  $\rho_{300\text{K}}(p)$ , decreases monotonously upon increasing pres-

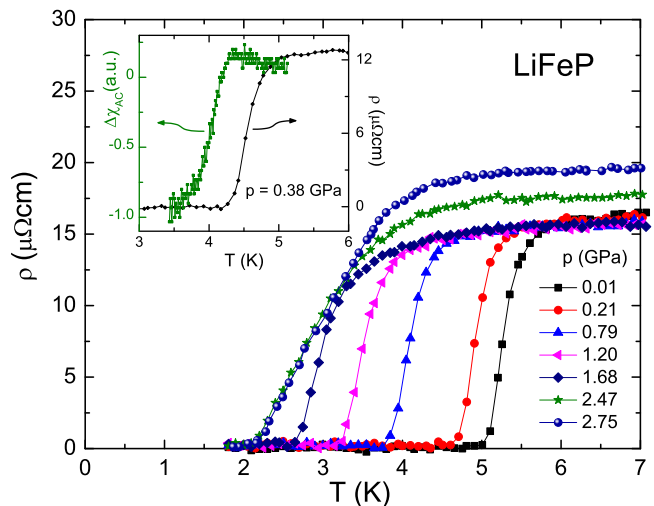


FIG. 2: Low-temperature electrical resistivity of LiFeP as function of temperature for different pressures as indicated. The inset displays the AC susceptibility and the electrical resistivity at  $p = 0.38 \text{ GPa}$  in the temperature region around the superconducting transition.

sure. This is also evidenced by the strong increase of the ratio  $\rho_0(p)/\rho_{300\text{K}}(p)$  (see lower inset in Fig. 1).

In addition to  $\rho(T)$  we measured  $\chi_{\text{AC}}(T)$  on the same sample and at the same pressures.  $\chi_{\text{AC}}(T)$  exhibits a narrow, step-like feature at the superconducting transition.  $\rho(T)$  reaches zero right at the temperature where  $\chi_{\text{AC}}(T)$  exhibits the onset of the diamagnetic response. Above  $p = 0.79 \text{ GPa}$ ,  $T_c$  drops out of our measurement window for  $\chi_{\text{AC}}$ . The inset of Fig. 2 shows  $\chi_{\text{AC}}(T)$  and, for comparison,  $\rho(T)$  at  $p = 0.38 \text{ GPa}$ . The evolution of  $T_c$  with increasing  $p$  is depicted in Fig. 3. The narrow width of the superconducting transition in resistivity and, further, the good correspondence between  $T_c$  determined by the  $\rho(T)$  and the  $\chi_{\text{AC}}(T)$  in the  $T - p$  phase diagram is unusual for superconductivity in stoichiometric “1111” and “122” materials. There, quite often zero resistance is found without any indication for bulk superconductivity or a very broad transition is observed (e.g. Ref. 25,26).

To determine the superconducting upper-critical field,  $H_{c2}(T)$ , we conducted measurements of the electrical resistivity in magnetic fields.  $H_{c2}$  vs.  $T$  curves at different pressures are displayed in Fig. 4.  $H_{c2}(T)$  exhibits a roughly linear temperature dependence in the accessible temperature range ( $T \geq 1.8 \text{ K}$ ) with the exception of the first data point in magnetic field ( $\mu_0 H = 0.5 \text{ T}$ ), which indicates the presence of a small tail. A similar tail has been previously reported in other iron-based superconductors.<sup>27-29</sup> As possible origin of the tail multi-band effects were discussed. Increasing pressure suppresses  $H_{c2}(T)$  effectively and, correspondingly, the absolute value of the slope  $\mu_0 dH_{c2}(T)/dT$  of a straight-line fit to the data decreases from  $1.92 \text{ T/K}$  at  $0.01 \text{ GPa}$  to  $0.95 \text{ T/K}$  at  $1.42 \text{ GPa}$ . Furthermore, with increas-

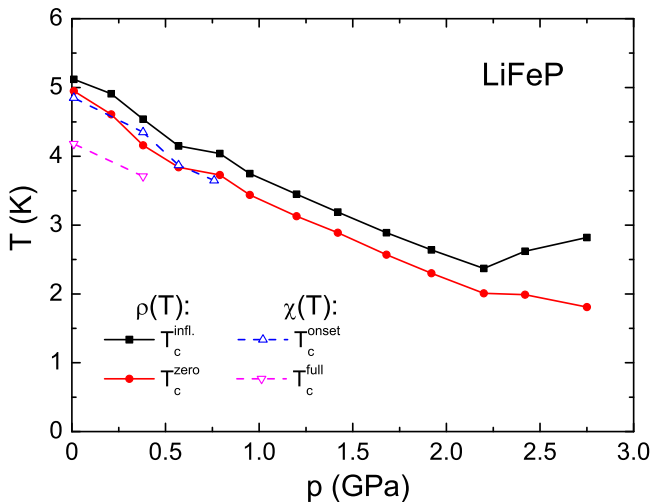


FIG. 3: Temperature - pressure phase diagram of LiFeP. The solid symbols correspond to results from  $\rho(T)$  measurements.  $T_c^{\text{infl.}}$  is defined by the inflection point of  $\rho(T)$  and  $T_c^{\text{zero}}$  by the temperature where zero resistivity is obtained. The open symbols correspond to  $T_c$  determined by  $\chi_{AC}(T)$  experiments.  $T_c^{\text{onset}}$  marks the onset of the diamagnetic response and  $T_c^{\text{full}}$  the full transition.

ing magnetic field the superconducting transition in  $\rho(T)$  gradually broadens as shown for  $p = 0.01$  GPa in the inset of Fig. 4. The broadening of the resistive transition on increasing magnetic field indicates an anisotropy of  $H_{c2}(T)$  as anticipated for a quasi-two-dimensional electronic structure.<sup>30</sup>

In comparison with LiFeAs, LiFeP can be viewed as *compressed* LiFeAs. At 5.5 – 6.5 GPa  $T_c$  of LiFeAs matches  $T_c$  of LiFeP at atmospheric pressure: LiFeAs “becomes” LiFeP.<sup>23,24,31</sup> The lattice parameters obtained for LiFeP are  $a = 3.692$  Å,  $c = 6.031$  Å<sup>22</sup> compared to  $a = 3.670$  Å,  $c = 6.108$  Å for LiFeAs at 6.54 GPa.<sup>23</sup> The lattice parameters  $a$  and  $c$  in LiFeAs are contracted by 2.7% and 3.9%, respectively, at 6.54 GPa, whereas the replacement of As by P reveals a highly anisotropic contraction of  $a$  and  $c$  by 2.1% and 5.1%, respectively. This leads to a smaller structural anisotropy in LiFeP compared to LiFeAs at 6.54 GPa. It has been pointed out for the iron-pnictides that  $T_c$  attains maximum values when the  $[\text{FePn}_4]$ , where  $\text{Pn} = \text{P}, \text{As}$ , form a regular tetrahedron.<sup>11,12</sup> At ambient pressure the  $[\text{FeP}_4]$  tetrahedron of LiFeP is only slightly distorted with  $\alpha = 108.58^\circ$  and  $\beta = 109.92^\circ$ ,<sup>22</sup> while LiFeAs at 6.54 GPa possesses a highly distorted tetrahedron  $\alpha = 99.39^\circ$  and  $\beta = 114.70^\circ$ .<sup>23</sup> The bond angle of a regular tetrahedron is  $109.47^\circ$ . A nearly perfect  $[\text{FeP}_4]$  tetrahedron in LiFeP, but a highly distorted  $[\text{FeAs}_4]$  tetrahedron in LiFeAs and taking into account a similar  $T_c$  in both materials suggest that the perfectness of the  $[\text{FePn}_4]$  tetrahedron is not the determining property for the value of  $T_c$ . Moreover, our result suggests that changes in the DOS other than those strictly related to the perfectness of the  $[\text{FePn}_4]$  tetrahedron are governing the value

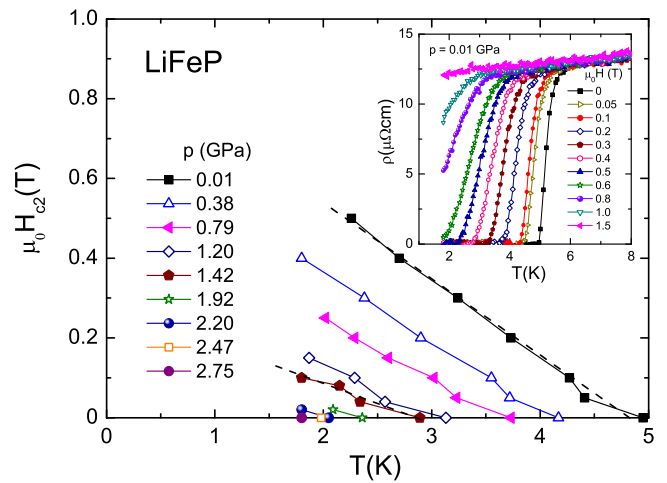


FIG. 4: Magnetic field - temperature phase diagram of LiFeP for different pressures. The dashed lines at  $p = 0.01$  and 1.42 GPa are serving as an example of the linear fits to the data. The inset shows the resistivity data for  $p = 0.01$  GPa for different magnetic fields. The zero-resistivity criterion was used for determining  $T_c$ .

of  $T_c$ . However, our experiments reveal that superconductivity in LiFeP is more robust than in LiFeAs. In LiFeAs  $T_c(p)$  decreases linearly on increasing pressure in the whole pressure range up to  $\sim 10$  GPa.<sup>24</sup> The initial slope of  $T_c(p)$   $|dT_c(p)/dp|_{p=0} = 1.23$  K/GPa for LiFeP is significantly smaller compared to the value in LiFeAs,  $|dT_c(p)/dp|_{p=0} = (1.56 \sim 2)$  K/GPa.<sup>23,31</sup> Since  $T_c(p)$  decreases linearly in LiFeAs, the same significant difference in the slopes of  $T_c(p)$  is present when we compare them where the  $T_c$ 's of LiFeP at  $p = 0$  and LiFeAs under pressure (5.5 – 6.5 GPa) are matching. This clearly indicates that the superconductivity in LiFeP is more robust than in LiFeAs. This is furthermore supported by a decreasing slope of  $T_c(p)$  upon increasing pressure in LiFeP (see Fig. 3). Therefore, our study suggests that a more regular  $[\text{FePn}_4]$  tetrahedron “strengthens” the superconducting state, but is not determining the size of  $T_c$ .

We will now turn to the unusual increase of the low-temperature normal-state resistivity above  $p \approx 2$  GPa. While the residual resistivity,  $\rho_0(p)$ , increases by about 1/3 from 1.68 GPa to 2.75 GPa, the  $A$  coefficient stays nearly pressure independent in this pressure range. This indicates that the QP-QP scattering rate does not change, but additional contributions to the residual scattering appear and become stronger upon increasing pressure. Since, as we discussed before,  $\rho_{300\text{K}}(p)$  decreases in the mentioned pressure range and, thus, we can exclude an extrinsic reason and, clearly, pressure does not add impurities, a different scattering mechanism has to be considered. An increase of  $\rho_0(p)$  is generally caused by additional disordered scattering centers. A similar increase of the resistivity at low temperatures is observed in LiFeAs, but at much higher pressures  $p \gtrsim 11$  GPa.<sup>24</sup> There, it

has been proposed that additional disordered scattering centers created by local magnetic ordering cause the enhanced  $\rho_0$ .<sup>24</sup> Increasing pressure reduces the in-plane Fe-Fe distance and concomitantly enhances local magnetic correlations leading to additional magnetic scattering centers.

In summary, we have studied the  $T - p$  phase diagram of the iron-pnictide superconductor LiFeP. Our experiments evidence a more robust superconducting state than

in the isostructural homolog LiFeAs. We relate this to the nearly regular  $[\text{FePn}_4]$  tetrahedron in LiFeP in contrast to the highly distorted one in LiFeAs. However we do not find a general relationship of the bond angle  $\alpha$  and  $T_c$  as suggested in literature.<sup>11</sup> Furthermore, we observe an enhanced QP-QP scattering rate at low pressures, which might indicate the presence of spin fluctuations. However further studies are needed to verify this speculation.

- 
- \* Electronic address: kamal@cpfs.mpg.de  
 † Electronic address: nicklas@cpfs.mpg.de
- <sup>1</sup> Y. Kamihara, H. Hiramatsu, M. Hirano, R. Kawamura, H. Yanagi, T. Kamiya, and H. Hosono, *J. Am. Chem. Soc.* **128**, 10012 (2006).
  - <sup>2</sup> T. Watanabe, H. Yanagi, T. Kamiya, Y. Kamihara, H. Hiramatsu, M. Hirano, and H. Hosono, *Inorg. Chem.* **46**, 7719 (2007).
  - <sup>3</sup> Y. Kamihara, T. Watanabe, M. Hirano, and H. Hosono, *J. Am. Chem. Soc.* **130**, 3296 (2008).
  - <sup>4</sup> X. H. Chen, T. Wu, G. Wu, R. H. Liu, H. Chen, and D. F. Fang, *Nature* **453**, 761 (2008).
  - <sup>5</sup> G. F. Chen, Z. Li, D. Wu, G. Li, W. Z. Hu, J. Dong, P. Zheng, J. L. Luo, and N. L. Wang, *Phys. Rev. Lett.* **100**, 247002 (2008).
  - <sup>6</sup> Z. A. Ren, J. Yang, W. Lu, W. Yi, G. C. Che, X. L. Dong, L. L. Sun, and Z. X. Zhao, *Mater. Sci. Innov.* **12**, 105 (2008).
  - <sup>7</sup> A. S. Sefat, M. A. McGuire, B. C. Sales, R. Jin, J. Y. Howe, and D. Mandrus, *Phys. Rev. B* **77**, 174503 (2008).
  - <sup>8</sup> H. Takahashi, K. Igawa, K. Arii, Y. Kamihara, M. Hirano, and H. Hosono, *Nature* **453**, 376 (2008).
  - <sup>9</sup> H. Takahashi, H. Okada, K. Igawa, Y. Kamihara, M. Hirano, H. Hosono, K. Matsubayashi, and Y. Uwatoko, *J. Supercond. Nov. Magn.* **22**, 595 (2009).
  - <sup>10</sup> G. Garbarino, P. Toulemonde, M. Álvarez-Murga, A. Sow, M. Mezouar, and M. Núñez-Regueiro, *Phys. Rev. B* **78**, 100507(R) (2008).
  - <sup>11</sup> C.-H. Lee, A. Iyo, H. Eisaki, H. Kito, M. T. Fernandez-Diaz, T. Ito, K. Kihou, H. Matsuhata, M. Braden, and K. Yamada, *J. Phys. Soc. Jpn.* **77**, 083704 (2008).
  - <sup>12</sup> J. Zhao, L. Wang, D. Dong, Z. Liu, H. Liu, G. Chen, D. Wu, J. Luo, N. Wang, Y. Yu, C. Jin, and Q. Guo, *J. Am. Chem. Soc.* **130**, 13828 (2008).
  - <sup>13</sup> F. Hardy, P. Adelmann, T. Wolf, H. v. Löhneysen, and C. Meingast, *Phys. Rev. Lett.* **102**, 187004 (2009).
  - <sup>14</sup> X. C. Wang, Q. Q. Liu, Y. X. Lv, W. B. Gao, L. X. Yang, R. C. Yu, F. Y. Li, and C. Q. Jin, *Solid State Commun.* **148**, 538 (2008).
  - <sup>15</sup> M. J. Pitcher, D. R. Parker, P. Adamson, S. J. C. Herkelrath, A. T. Boothroyd, R. M. Ibberson, M. Brunelli, and S. J. Clarke, *Chem. Commun.*, 5918 (2008).
  - <sup>16</sup> J. H. Tapp, Z. Tang, B. Lv, K. Sasmal, B. Lorenz, P. C. W. Chu, and A. M. Guloy, *Phys. Rev. B* **78**, 060505(R) (2008).
  - <sup>17</sup> D. R. Parker, M. J. Pitcher, P. J. Baker, I. Franke, T. Lancaster, S. J. Blundell, and S. J. Clarke, *Chem. Commun.*, 2189 (2009).
  - <sup>18</sup> C. de la Cruz, Q. Huang, J. W. Lynn, J. Y. Li, W. Ratcliff II, J. L. Zarestky, H. A. Mook, G. F. Chen, J. L. Luo, N. L. Wang, and P. C. Dai, *Nature (London)* **453**, 899 (2008).
  - <sup>19</sup> A. I. Goldman, D. N. Argyriou, B. Ouladdiaf, T. Chatterji, A. Kreyssig, S. Nandi, N. Ni, S. L. Bud'ko, P. C. Canfield, and R. J. McQueeney, *Phys. Rev. B* **78**, 100506(R) (2008).
  - <sup>20</sup> A. Jesche, N. Caroca-Canales, H. Rosner, H. Borrmann, A. Ormeci, D. Kasinathan, H. H. Klauss, H. Luetkens, R. Khasanov, A. Amato, A. Hoser, K. Kaneko, C. Krellner, and C. Geibel, *Phys. Rev. B* **78**, 180504(R) (2008).
  - <sup>21</sup> M. Rotter, M. Tegel, D. Johrendt, I. Schellenberg, W. Hermes, and R. Pöttgen, *Phys. Rev. B* **78**, 020503(R) (2008).
  - <sup>22</sup> Z. Deng, X. C. Wang, Q. Q. Liu, S. J. Zhang, Y. X. Lv, J. L. Zhu, R. C. Yu and C. Q. Jin, *EPL* **87**, 37004 (2009).
  - <sup>23</sup> M. Mito, M. J. Pitcher, W. Crichton, G. Garbarino, P. J. Baker, S. J. Blundell, P. Adamson, D. R. Parker, and S. J. Clarke, *J. Am. Chem. Soc.* **131**, 2986 (2009).
  - <sup>24</sup> S. J. Zhang, X. C. Wang, R. Sammynaiken, J. S. Tse, L. X. Yang, Z. Li, Q. Q. Liu, S. Desgreniers, Y. Yao, H. Z. Liu, and C. Q. Jin, *Phys. Rev. B* **80**, 014506 (2009).
  - <sup>25</sup> S. R. Saha, N. P. Butch, K. Kirshenbaum, and J. Paglione, and P. Y. Zavalij, *Phys. Rev. Lett.* **103**, 037005 (2009)
  - <sup>26</sup> M. Kumar, M. Nicklas, A. Jesche, N. Caroca-Canales, M. Schmitt, M. Hanfland, D. Kasinathan, U. Schwarz, H. Rosner, and C. Geibel, *Phys. Rev. B* **78**, 184516 (2008).
  - <sup>27</sup> Z.-S. Wang, H.-Q. Luo, C. Ren, and H.-H. Wen, *Phys. Rev. B* **78**, 140501(R) (2008).
  - <sup>28</sup> F. Hunte, J. Jaroszynski, A. Gurevich, D. C. Larbalestier, R. Jin, A. S. Sefat, M. A. McGuire, B. C. Sales, D. K. Christen, and D. Mandrus, *Nature* **453**, 903 (2008).
  - <sup>29</sup> C. F. Miclea, M. Nicklas, H. S. Jeevan, D. Kasinathan, Z. Hossain, H. Rosner, P. Gegenwart, C. Geibel, and F. Steglich, *Phys. Rev. B* **79**, 212509 (2009).
  - <sup>30</sup> S. Lebegue, *Phys. Rev. B* **75**, 035110 (2007).
  - <sup>31</sup> M. Gooch, B. Lv, J. H. Tapp, Z. Tang, B. Lorenz, A. M. Guloy, and P. C. W. Chu, *EPL* **85**, 27005 (2009).